7. Chapter 7: A solid solution approach to enable easier and reliable integration of SBT based capacitors into high density FRAMs.

7.1 Abstract

We report on $(SrBi_2Ta_2O_9)_{1-x}(Bi_3TiNbO_9)_x$ solid solution thin films with enhanced ferroelectric properties at a low processing temperature of 650^0 C as compared to $SrBi_2Ta_2O_9$. Polycrystalline thin films with layered perovskite structure were successfully fabricated by metalorganic solution deposition technique on Pt substrates. The effects of Bi_3TiNbO_9 (BTN) content on the microstructure, dielectric and ferroelectric properties were analyzed as a function of x (0.0-1.0) and annealing temperatures (650-750^0 C) to identify the optimum composition for high density FRAM applications. With the addition of BTN ($x \leq 0.4$) to SBT, the grain size and the ferroelectric properties were significantly enhanced, as compared to pure SBT thin films. In addition, processing temperature was lowered considerably while maintaining the excellent fatigue and retention characteristics of SBT. Thin films with optimum composition ($SBT_{0.8}BTN_{0.2}$) exhibited typical P_r and E_c values of 7.0 $\mu C/cm^2$ and 75 kV/cm, respectively, at an annealing temperature of 650^0 C while the leakage current density was less than 10^{-8} A/cm^2 at an applied field of 250 kV/cm. It was possible to decrease the coercive voltage to 0.8V by decreasing the film thickness to 100nm. Thin films of the solid solution material with improved microstructure and ferroelectric properties show a great promise to solve major problems with SBT based capacitor technology for FRAM applications.

7.2 Introduction

Ferroelectric thin films are being widely investigated for non-volatile memory applications[1,2]. Ferroelectric memory technology offers significant improvement compared to the present commercial non-volatile memory technologies, such as faster switching speeds, low operating voltages and high endurance[2-5]. Among the ferroelectric materials, $SrBi_2Ta_2O_9$ is one of the most promising materials for non-volatile memory devices because of it's fatigue free nature[6-8] on metal electrodes such as platinum. However, SBT based memory technology has to overcome the problems of high processing temperature (≥ 750 ^{0}C), low remanent polarization (P_r) and low Curie temperature (T_c = 310 ^{0}C) for the realization of a practical high density ferroelectric random access memories (FRAMs). For high density memories, the SBT thin film is required to be integrated directly on poly-Si plug[9]. Hence, a low processing temperature is desirable to inhibit the interdiffusion of Si and electrode/ferroelectric material, and maintain good interfacial characteristics. Additionally, it is necessary to improve the P_r and T_c characteristics of SBT while attempting to reduce the processing temperature, for high density memories with small cell structures and high temperature applications[10].

Several techniques such as MOD[6,7,10], MOCVD[11], sputtering[13] and laser ablation[8] have been used for the deposition of SBT thin films. All these reports have shown that annealing temperature greater than 750 ^{0}C was necessary to get good ferroelectric properties, however, the crystalline phase formation occurred at temperatures far lower than that at which good ferroelectric properties were observed. This trend was attributed to the critical effect of grain size and orientation on the ferroelectric properties of SBT thin films[12]. It has been established that a critical grain size is necessary to get good

ferroelectric properties in SBT thin films which necessitated an annealing temperature of 750 ^{0}C[13,14]. For successful integration into high density memories, in addition to low processing temperature, an improvement in P_r and T_c is required. SBT has been observed to exhibit low P_r inherently, which follows the linear T_c-P_s relationship[16] for layered ferroelectric compounds.

$$T_c = 418 + 17.7\ P_s \qquad (1)$$

Accordingly, layered perovskite materials with high Tc were found to exhibit higher polarization charge. Based on the above mentioned reasons, it could be concluded that a low processing temperature and high P_r could be achieved in SBT thin film by increasing the grain size and T_c. There were few reports on reducing the processing temperature of SBT. Attempts were previously made by the addition of donors, acceptors, excess Bi_2O_3 and by annealing in low O_2 partial pressures[17,18] However, there were no significant improvements in grain size and ferroelectric property. In the present work, a solid solution approach is taken to improve the microstructure and ferroelectric properties of SBT thin films in an attempt to reduce it's processing temperature.

Solid solution approach is commonly used in bulk ceramics to modify the properties of a material by making a solid solution with another material possessing different microstructural and electrical characteristics. In the present study, a successful attempt was made to increase the grain size at low processing temperatures, by choosing a solid solution approach, because a solid solution would enhance the diffusion constants of the individual species at a given temperature and hence, enable a larger grain size at low annealing temperatures. In addition, a simultaneous increase in P_r and T_c would be possible by choosing a ferroelectric material possessing high Curie temperature as the

solute. It was found that layered ferroelectric materials constituting atoms with higher electronegativity possessed higher Curie temperature. However, in order to achieve a solid solution, it is necessary to choose a solute ferroelectric material with same crystal structure and similar lattice parameters as SBT. SBT belongs to the Aurivillius family of bismuth layered structure compounds of the general formula of (Bi_2O_2)-$(M_{n-1}R_nO_{3n+1})$ where M = Ba, Pb, Sr, Bi, K or Na, n = 2, 3, 4 or 5 and R =Ti, Nb or Ta. SBT has orthorhombic symmetry with the structure comprised of a number of perovskite-like units of nominal composition MRO_3 between Bi_2O_2 layers along the orthorhombic c-axis[19-22]. Table 7.1 illustrates the Curie temperatures of possible bismuth layered ferroelectric compounds as against the electronegativity of the substituting atom. Owing to it's high Curie temperature, Bi_3TiNbO_9 (BTN) was selected as the solute ferroelectric material to form a solid solution with SBT. Initially, the work was done on bulk samples to establish that SBT and BTN form a complete solid solution for all the ratios of SBT and BTN, and that grain size and T_c, increase with an increase of BTN content in the solid solution of $(SBT)_{1-x}(BTN)_x$[23].

In this paper we report on the detailed structural and ferroelectric properties of the thin films of $(SBT)_{1-x}(BTN)_x$ solid solution. The effects of BTN content (0-100%) and processing temperature on the properties of solid solution films were analyzed to identify an optimum composition for FRAM applications.

Table 7.1 Curie Temperature of (T_c) of layered ferroelectric compounds as a function of electronegativity of the substituting atoms

Compound	**T_c**	**Electronegativity (kJ/g-at)**
$BiBi_2TiNbO_9$	1220 K	819
$CaBi_2Nb_2O_9$	920 K	575
$PbBi_2Nb_2O_9$	830 K	714
$SrBi_2Nb_2O_9$	700 K	525
$BaBi_2Nb_2O_9$	470 K	483
$BiBi_2TiTaO9$	1140 K	819
$CaBi_2Ta_2O_9$	870 K	575
$PbBi_2Ta_2O_9$	700 K	714
$SrBi_2Ta_2O_9$	600 K	525
$BaBi_2Ta_2O_9$	370 K	483

7.3 Experimental

Thin films of $(SBT)_{1-x}(BTN)_x$ solid solutions were prepared by a modified metalorganic solution deposition method[24] (Fig. 7.1). Bismuth 2-ethyl hexanoate (Alfa Aesar), titanium isopropoxide (Alfa Aesar), strontium acetate (Alfa Aesar), tantalum ethoxide (Inorg Tech) and niobium ethoxide (Inorg Tech) were used as precursors. 2-ethyl hexanoic acid, 2-methoxy ethanol and acetic acid were selected as the solvents. 0.125M solutions were prepared for compositions with the general formula of $(SBT)_{1-x}$ $(BTN)_x$ with x varying from 0.0 to 1.0. Initially, clear solutions of bismuth 2-ethyl hexanoate in hexanoic acid, strontium acetate in acetic acid, tantalum and niobium ethoxides in 2-methoxy ethanol were prepared separately. These three solutions were mixed together to obtain a transparent solution. Titanium isopropoxide was finally added and the solution was stirred for about two hours. The solution was coated on to $Pt/TiO_2/SiO_2/Si$ substrates using a spin coater at a speed of 6000 rpm. After each coating the films were pyrolized on a hot plate at a temperature of 200 ^{0}C for two minutes. Seven layers were coated to achieve a final thickness of 0.25 μm. Post deposition annealing of the films was carried out in a conventional furnace at temperatures ranging from 650-750 ^{0}C in an oxygen atmosphere for one hour. Top electrodes were deposited by sputtering Pt through a shadow mask on the top surface of the thin films to form metal-ferroelectric-metal (MFM) capacitors. These capacitors were given a second annealing for 20 minutes at the same temperatures as that of the first anneal.

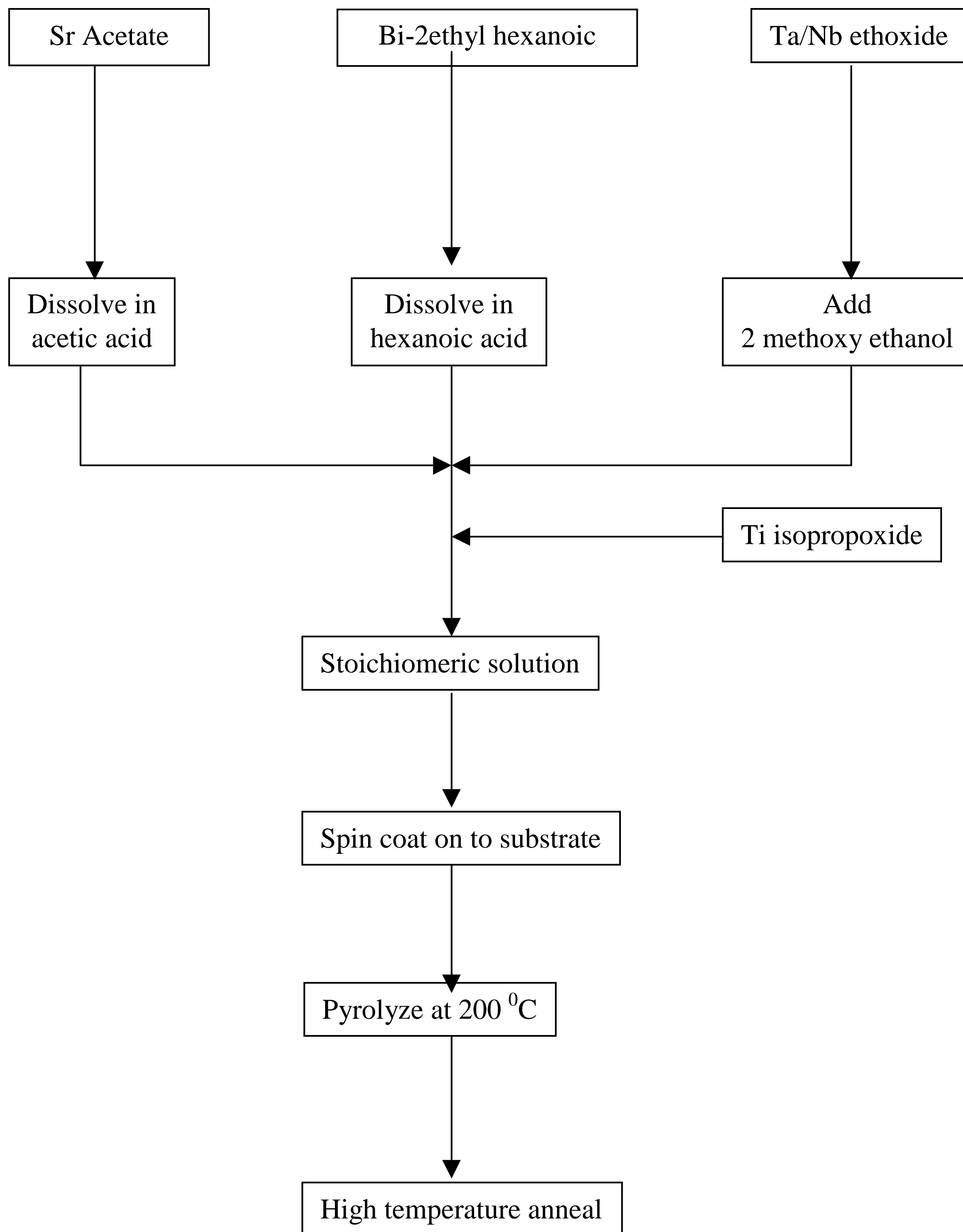

Fig. 7.1. Metalorganic solution deposition process of $(SBT)_{1-x}$ $(BTN)_x$ thin films

X-ray diffraction analyses were conducted on the present films using a SCINTAG DMS 2000 diffractometer with Cu K_{α} radiation (λ = 1.54056 Å) at a scanning speed of 2° (2θ)/min. Digital Instruments D3000 Atomic Force Microscope (AFM) was used to study the surface morphology. The dielectric measurements were conducted on MFM capacitors with HP 4192A impedence analyzer at room temperature. The dielectric properties were measured in terms of the dielectric constant (ε_r) and loss factor (tan δ). P-E hysteresis measurements were conducted at room temperature on $(SBT)_{1-x}(BTN)_x$ thin films in MFM configuration using standardized RT66A ferroelectric test system. DC leakage current was determined using a Keithley 617 programmable electrometer/source.

7.4 Results and Discussion

In the present paper, we report on the structure and ferrroelectric properties of the $(SBT)_{1-x}(BTN)_x$ solid solution thin films deposited on the $Pt/TiO_2/SiO_2/Si$ substrates. The effects of BTN content on the properties of the solid solution thin films have been analyzed. The film properties were found to be strongly dependent on the post-deposition annealing temperature. An optimum composition for high density FRAM application was identified based on the results of these studies. The properties of the optimum composition solid solution thin films at a low processing temperature of 650 ^{0}C have been analyzed in detail.

Fig. 7.2 shows the x-ray diffraction patterns of the $SBT_{(1-x)}BTN_x$ solid solution thin films (x = 0.0 to 1.0) annealed at 700 ^{0}C in an oxygen atmosphere. It was observed that all the films crystallized predominantly in orthorhombic single phase. There were no detectable second phases indicating a complete reaction. As the amount of BTN in the solid solution was increased, a progressive shift in the peaks towards higher 2θ values was observed. Similar results were obtained earlier[23] for the bulk samples of solid solution. This shift in the peaks could be explained on the basis of gradual distortion of the unit cell with increasing BTN content. However in the bulk samples a split in the peaks of (020, 200) and (224, 0014) orientation was observed for BTN contents ≥ 60%, which is due to large difference between a and b lattice parameters of the unit cell. In the case of thin films, no such split in the peaks was noticed, instead a slight broadening of the peaks of (020, 200) and (224,0014) was observed for the compositions with BTN content more than 60%.

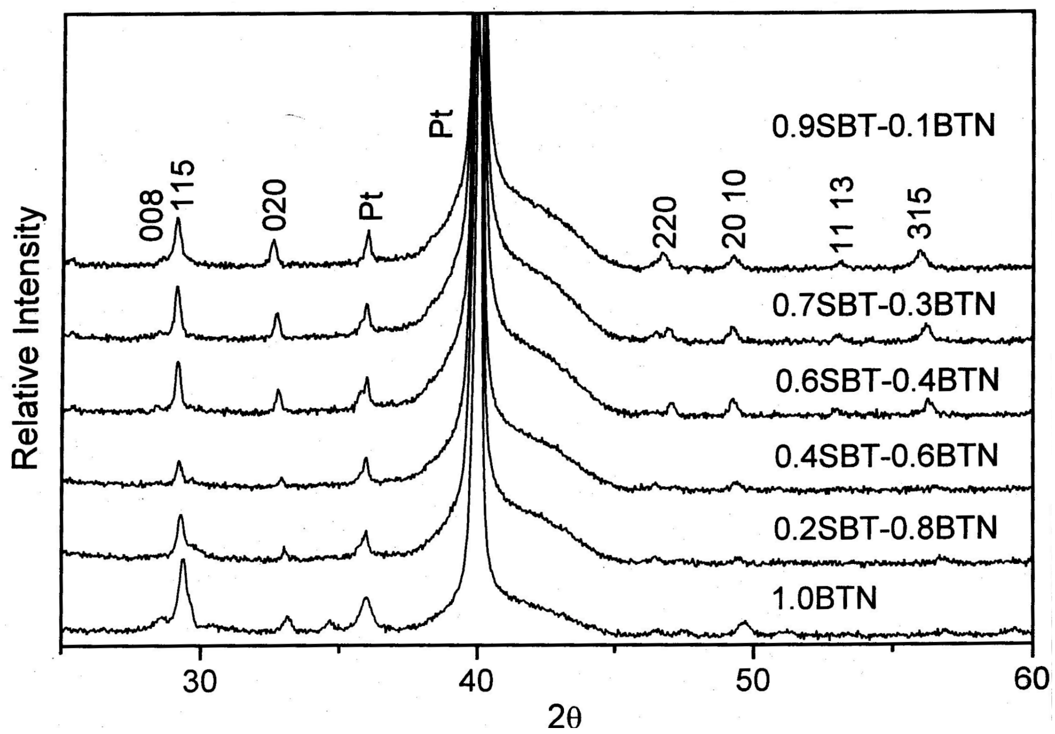

Fig. 7.2. XRD patterns of $(SBT)_{1-x}(BTN)_x$ thin films annealed at 700 ^{0}C for one hour.

Apart from the XRD patterns, formation of well crystallized films was also indicated by the surface morphology of the thin films. Fig. 7.3 shows the AFM micrographs (1μm×1μm dimension) of $(SBT)_{1-x}(BTN)_x$ thin films with x varying from 0.0 to 1.0. All the films were annealed at 700 ^{0}C for one hour in an oxygen atmosphere. A very well crystallized, fairly uniform grain structure could be seen in the topography. Table 7.2 gives the average surface roughness of the films which is the mean value of the surface relative to the center plane calculated using a least squares program. It was found that the average surface roughness of all the films was less than 7 nm indicating a very smooth surface morphology. The average grain size varied from 50 nm to 300 nm. In the range x = 0.0 to 0.4, the average grain size increased with the increase in BTN content in the solid solution. This increase in the grain size could be attributed to the increase in mobility of the species forming the solid solution with the addition of BTN. An important observation was that the average grain size of all the films in this composition range was significantly greater, as expected, than that obtained in case of SBT at the same processing temperature of 700 ^{0}C[14]. However, in the range x =0.5 to 1.0, the average grain size dropped to less than 60 nm.

Ferroelectric hysteresis measurements were conducted on 0.25-μm-thick solid solution films which were annealed at 650 ^{0}C, 700 ^{0}C and 750 ^{0}C for one hour. Ferroelectric P-E hysteresis loops were measured at an applied field of 200 kV/cm. Fig. 7.4 shows the remanent polarization as a function of BTN content for each annealing temperature. The remanent polarization values were found to be significantly improved compared to SBT thin films. For instance, P_r of 70%SBT:30%BTN thin films annealed at 650 ^{0}C was found to be about 7.0 μC/cm^2, while pure SBT thin film processed at the

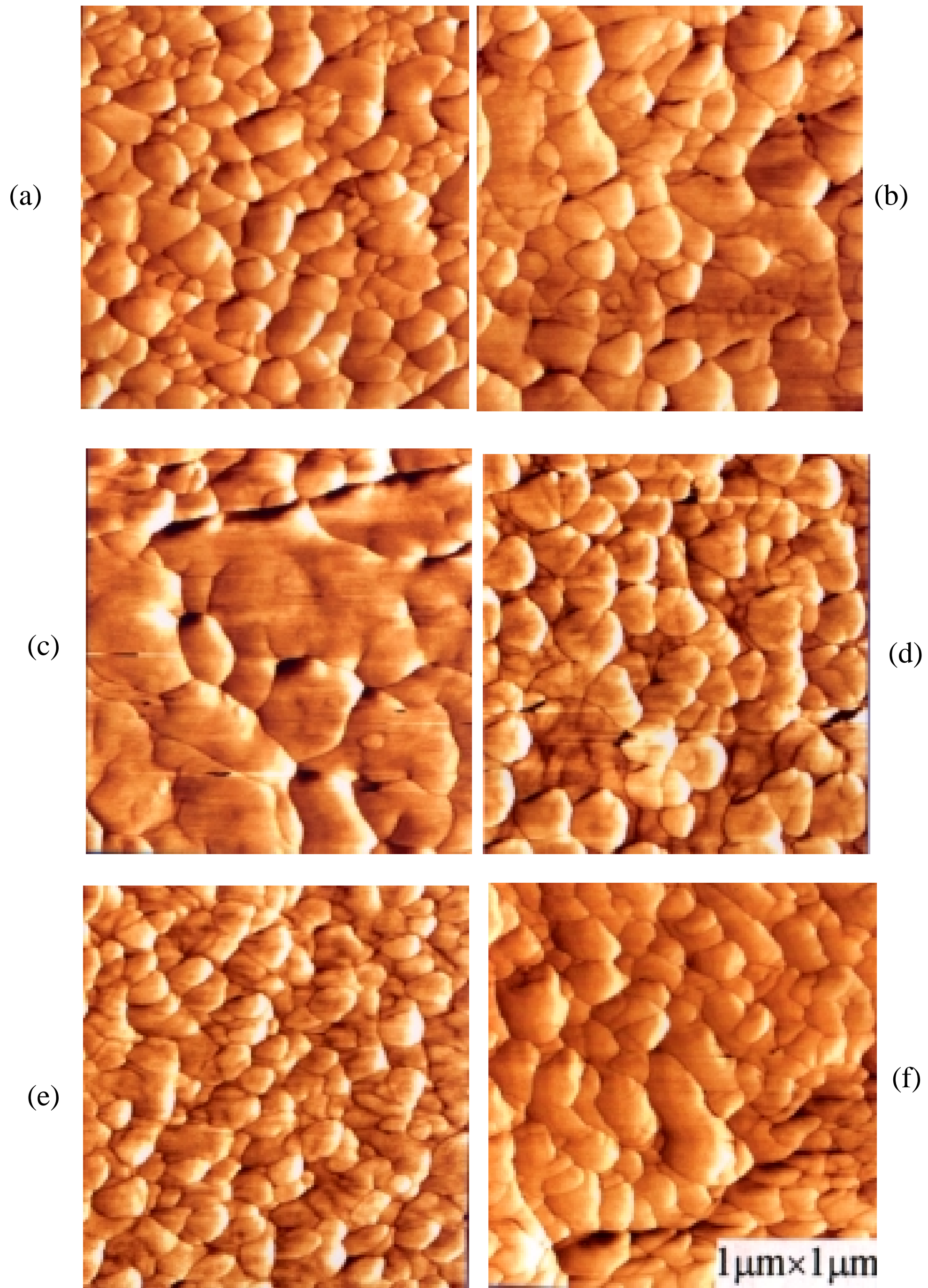

Fig. 7.3 AFM photographs of $(SBT)_{1-x}$ $(BTN)_x$ thin films annealed at 700 ^{0}C for one hour. (a) x = 0.1, (b) x = 0.3, (c)x = 0.4, (d) x = 0.6, (d) x = 0.8 and (f) x = 1.0

Table 7.2 Mean Roughness of the films annealed at 700 ^{0}C/1 Hr as a function of amount of BTN (x) in the solid solution of $(SBT)_{1-x} (BTN)_x$.

x	**Mean Roughness (nm)**
0.1	5.2
0.3	6.3
0.4	6.1
0.6	6.5
0.8	6.9
1.0	8.7

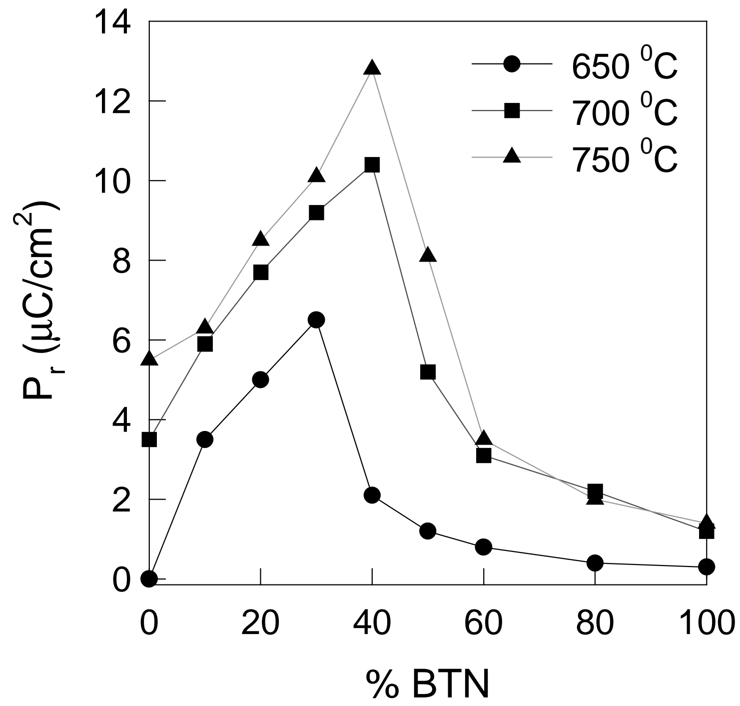

Fig 7.4 Remanent polarization (P_r) of $(SBT)_{1-x}(BTN)_x$ thin films annealed at various temperatures as a function of amount of BTN

same temperature did not show any hysteresis loop at all. For BTN contents up to 40%, P_r was found to increase with the increase in BTN amount in $(SBT)_{1-x}(BTN)_x$ solid solution, with a maximum P_r value of 10 $\mu C/cm^2$ and 12 $\mu C/cm^2$ attained in the thin films of $SBT_{0.6}BTN_{0.4}$ annealed at 700 ^0C and 750 ^0C respectively, while SBT thin films processed at the same temperatures exhibited a much lower P_r of 3.9 $\mu C/cm^2$ and 5.9 $\mu C/cm^2$, respectively. It was expected because of considerable increase in the grain size with the addition of BTN, as seen in AFM micrographs (Fig. 7.3)[12]. However, on further addition of BTN (>40%), P_r was found to decrease with increasing BTN content due to formation of smaller grains (Fig. 7.3). It appears at this point that each composition of $(SBT)_{1-x}(BTN)_x$ solid solution might possess a critical grain size necessary to exhibit good ferroelectric properties, as is the case in SBT thin films[14]. This also explains the shift of P_r versus BTN content curve (Fig. 7.4) to the lower BTN percentages in the $(SBT)_{1-x}(BTN)_x$ thin films annealed at 650 ^0C because we would expect smaller grain sizes for the films processed at 650 ^0C as compared to the films annealed at 700 ^0C or 750 ^0C.

Fig. 7.5 shows the effect of BTN content on the coercive field of $(SBT)_{1-x}(BTN)_x$ thin films. Though remanent polarization increased with the addition of BTN, for BTN contents up to 40% (for the films annealed at 700 ^0C and 750 ^0C), coercive field was also found to increase simultaneously. In fact, coercive field followed the same trend as that of P_r when plotted as a function of composition as shown in Fig. 7.5. The maxima in E_c vs BTN content were observed at 60%SBT:40% BTN for films annealed at 700 ^0C and 750 ^0C with magnitudes of 65 kV/cm and 73 kV/cm, respectively. For films annealed at 650 ^0C, the maximum occurred at 30% BTN content bearing a value of 86 kV/cm.

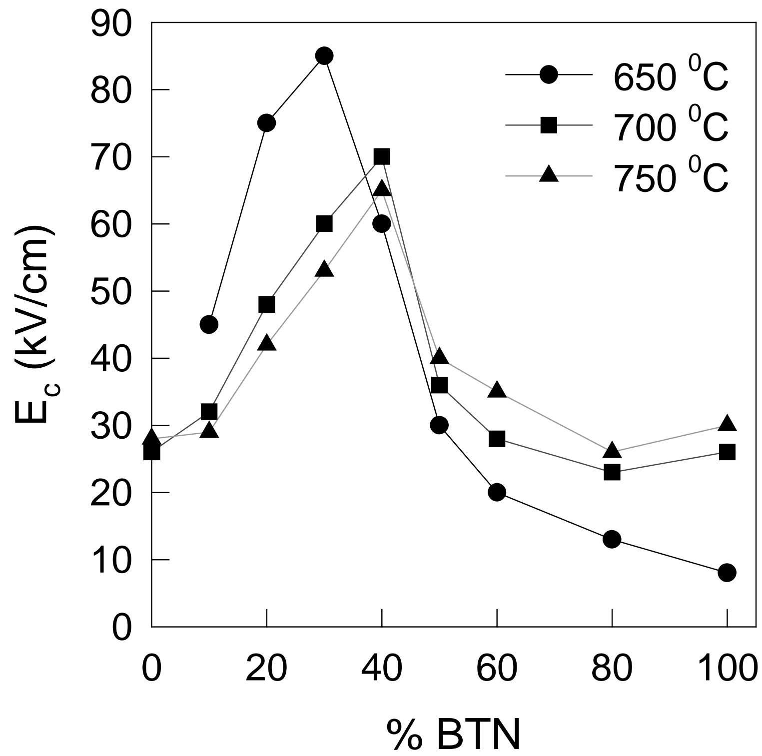

Fig 7.5 Coercive field (E_c) of $(SBT)_{1-x}(BTN)_x$ thin films annealed at various temperatures as a function of amount of BTN

Although coercive field of these films was high, the coercive voltage ($V_c \cong E_c \times$ thickness), which is of practical importance to the semiconductor industry, could be decreased by decreasing the thickness of the thin films and is discussed later.

Thin films of $SBT_{(1-x)}BTN_x$ in the range x = 0.1 to 1.0, annealed at 650 ^{0}C, 700 ^{0}C and 750 ^{0}C, were investigated to analyze the effects of BTN content in the solid solution on the dielectric properties and the nature of electrode/film interface. Dielectric properties were measured in terms of relative permittivity (ε_r) and dielectric loss (tan δ) by applying a small ac signal of 10 mV across the sample. The permittivity showed no dispersion with frequency up to 1 MHz indicating that the values obtained were not masked by any surface layer effects or barrier effects in the measured frequency range. Hence the permittivity measured at a frequency of 100 kHz was used to study the dependence of ε_r on the composition of $(SBT)_{1-x}(BTN)_x$ thin films. Fig. 7.6 shows the dielectric constant as a function of BTN content for each annealing temperature. Dielectric constants of all these compositions were found to be vary between 80-220 and were found to be less than that of SBT. This obeyed the argument that any addition of BTN, which has a lower dielectric constant as compared to that of SBT[27], would decrease the dielectric constant of the solid solution formed by SBT and BTN. As a result, the maximum value of $\varepsilon_{r,}$ which was observed at 40% BTN content in the $(SBT)_{1-x}(BTN)_x$ thin films annealed at 750 ^{0}C, was found to be 210 which is much smaller than the value of 330 reported for SBT thin films[28]. Also, dielectric constant ε_r showed a maximum at 40% BTN content for the solid solution films annealed at 700 ^{0}C, while the $(SBT)_{1-x}(BTN)_x$ thin films annealed at 650 ^{0}C exhibited the highest value of ε_r at 30% BTN. This trend was similar to the one shown by the P_r and E_c when plotted as a function of

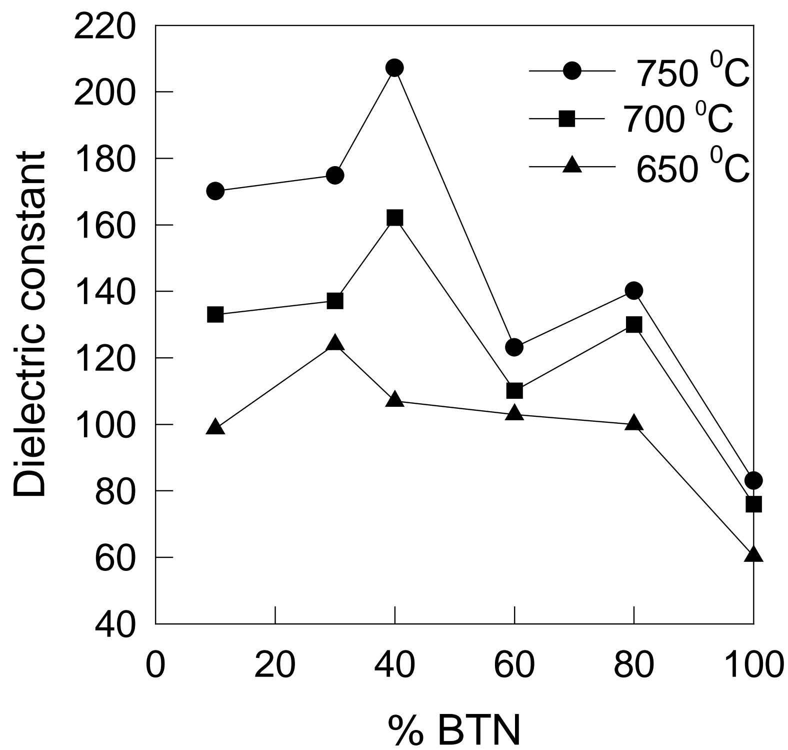

Fig 7.6 Dielectric constant of $(SBT)_{1-x}(BTN)_x$ thin films annealed at various temperatures as a function of amount of BTN

composition for each annealing temperature (Fig. 7.4 and Fig. 7.5). Such a behavior could be attributed to the grain size dependence on the composition and annealing temperature.

Leakage current is an important parameter in the device application. SBT is an attractive material for device applications because of it's very low leakage current density even in very thin films (<0.1 μm). The leakage currents in the MFM capacitors of $SBT_{(1-x)}BTN_x$ solid solution thin films were measured at room temperature as a function of x at an applied field of 100 kV/cm. Fig. 7.7 shows the leakage current density as a function of amount of BTN in these thin films. The leakage current density of the solid solution thin films was comparable to that of SBT thin films, even though the grain size was much larger than that of SBT thin film. It could be observed that the leakage current densities of the thin film capacitors (except 100% BTN) were lower than 10^{-7} A/cm^2. However, the leakage current density increased by a small magnitude with increase in the amount of BTN. While holding all the processing parameters constant, the increase in the leakage current could be attributed to the increase in Nb content with the addition of BTN to the $(SBT)_{1-x}(BTN)_x$ solid solution system. The defects caused by the presence of Nb, which exhibits two stable valency states (3 and 5), add to any pre-existing defects in the capacitor to increase the net leakage current density.

Layered perovskite materials are attractive for FRAM applications because of their fatigue free characteristics on metal electrodes. SBT thin films have been shown to possess good fatigue properties up to 10^{12} switching cycles. The switching endurance of 0.25-μm-thick $(SBT)_{1-x}(BTN)_x$ capacitors annealed at 700 ^{0}C was studied as a function of x varying from 0.0 to 1.0. This was done by applying 10^{10} switching cycles of 8.6-μs-

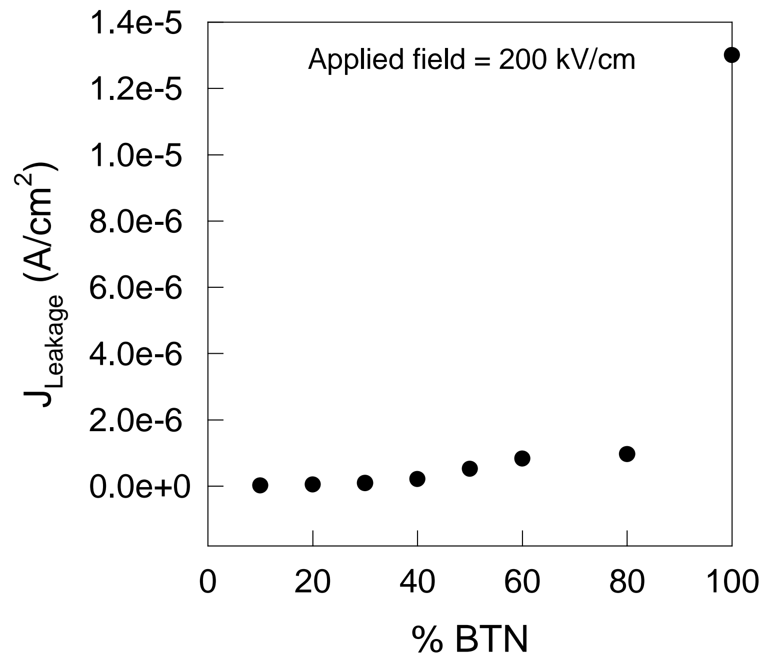

Fig 7.7 Leakage current density (I_L) of $(SBT)_{1-x}(BTN)_x$ thin films annealed at various temperatures as a function of amount of BTN

wide bipolar pulses of 5 V amplitude and 500 kHz frequency. Fig. 7.8 illustrates the dependence of fatigue property of these capacitors as a function of BTN content in the solid solution. Although P_r and E_c of the $(SBT)_{1-x}(BTN)_x$ thin film capacitors was high (as compared to SBT thin films processed at the same temperature), these MFM capacitors exhibited excellent fatigue properties. Even after 10^{10} cycles, the decay in P_r was observed to be less than 5% of the initial value owing to the inherent fatigue free nature of these bismuth layered perovskites.

Based on the ferroelectric, leakage current and fatigue properties of $(SBT)_{1-x}(BTN)_x$ solid solution thin films, an optimum composition suitable for high density FRAMs was found to be 80%SBT:20%BTN. 0.25 μm thick 0.8SBT-0.2BTN solid solution thin film annealed at 650 ^{0}C for one hour exhibited a well saturated P-E hysteresis loop as shown in Fig. 7.9. The remanent polarization and coercive voltage were found to be 5.0 μC/cm^2 and 70 kV/cm, respectively. This is a significant improvement compared to SBT thin films annealed at 650 ^{0}C which exhibited no distinct hysteresis loop at all. Fig. 7.10 gives the leakage current density of 0.8SBT-0.2BTN thin films as a function of the applied field. It was observed that even at an applied field of 250 kV/cm, the leakage current density was as lower than 2×10^{-9} A/cm^2 which was comparable to that of SBT thin films. Fig. 7.11 illustrates the fatigue characteristics of 0.8SBT-0.2BTN thin films measured by applying 10^{11} cycles of 8.6-μs-wide bipolar pulses of 5 V amplitude and a frequency of 500 kHz. No polarization fatigue was observed even after 10^{11} cycles. All these excellent properties of the solid solution thin films show great promise to solve major problems with SBT based capacitor technology for FRAM applications.

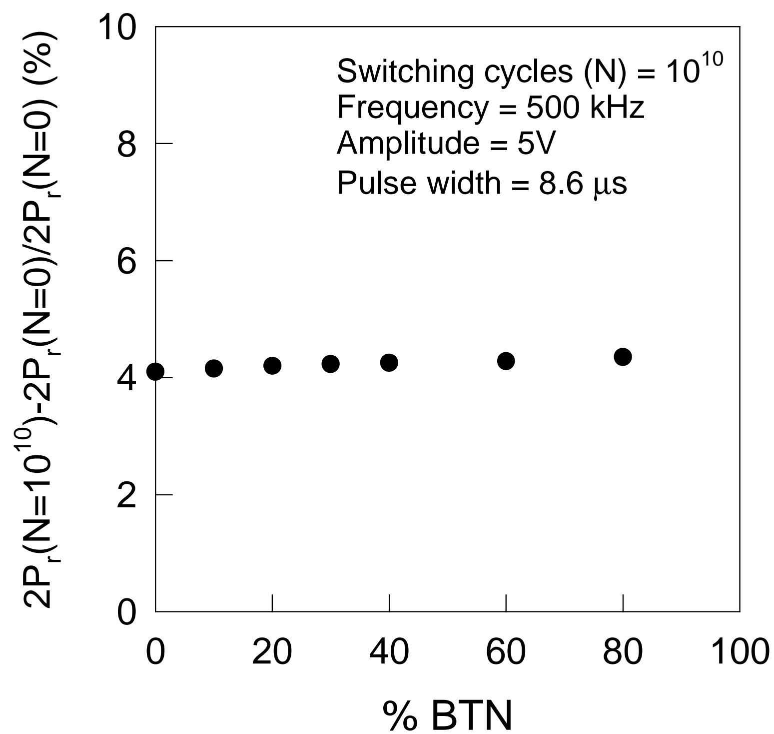

Fig 7.8 Fatigue characteristics of $(SBT)_{1-x}(BTN)_x$ thin films annealed at various temperatures as a function of amount of BTN

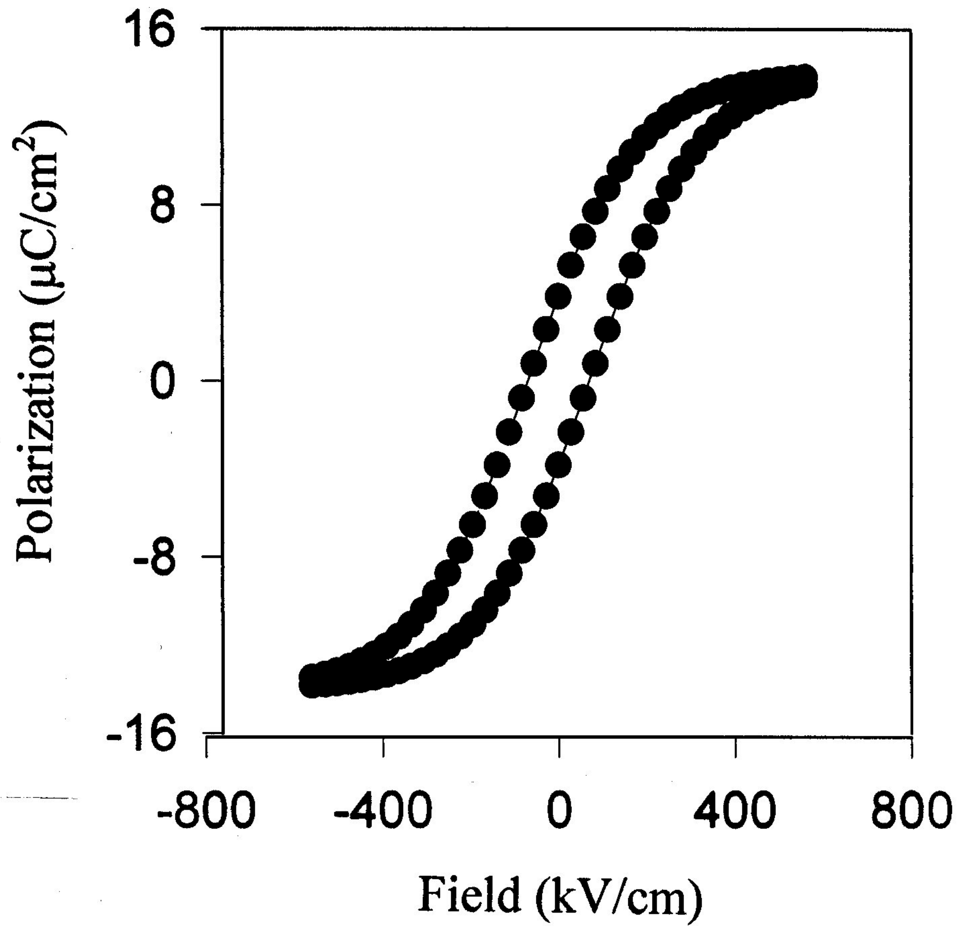

Fig. 7.9. Hysteresis loop of 0.25-μm-thick $(SBT)_{0.8}(BTN)_{0.2}$ thim film annealed at 650 ^{0}C for one hour.

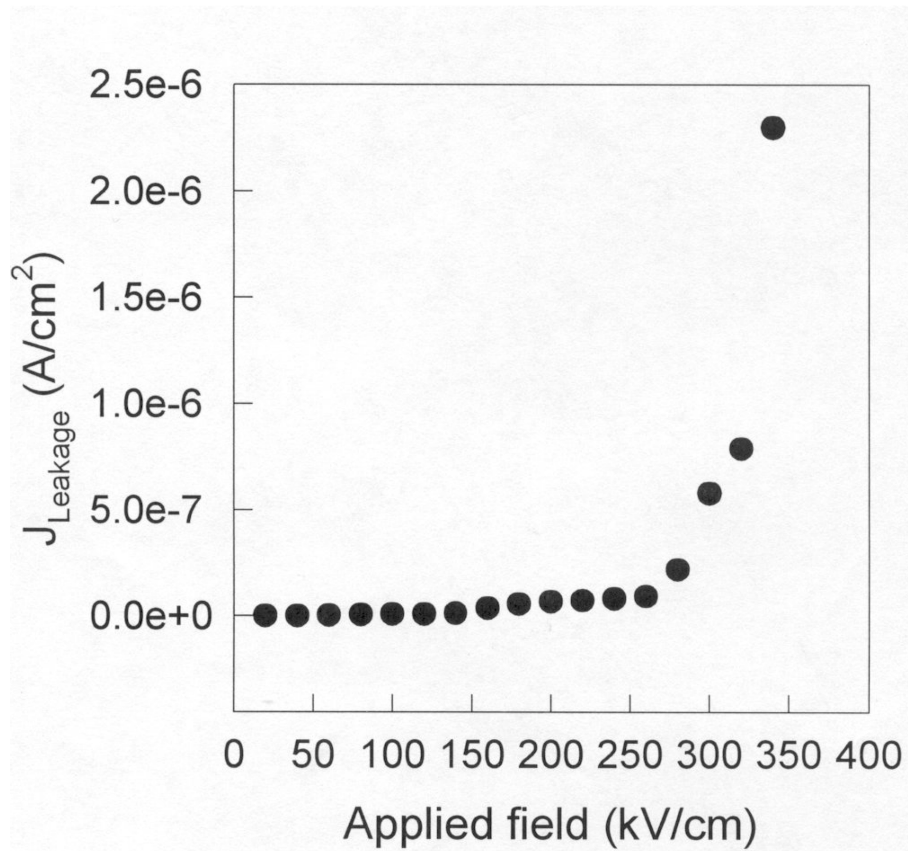

Fig. 7.10. Leakage current density of 0.25-μm-thick $(SBT)_{0.8}(BTN)_{0.2}$ thim film annealed at 650 ^{0}C for one hour as a function of applied field.

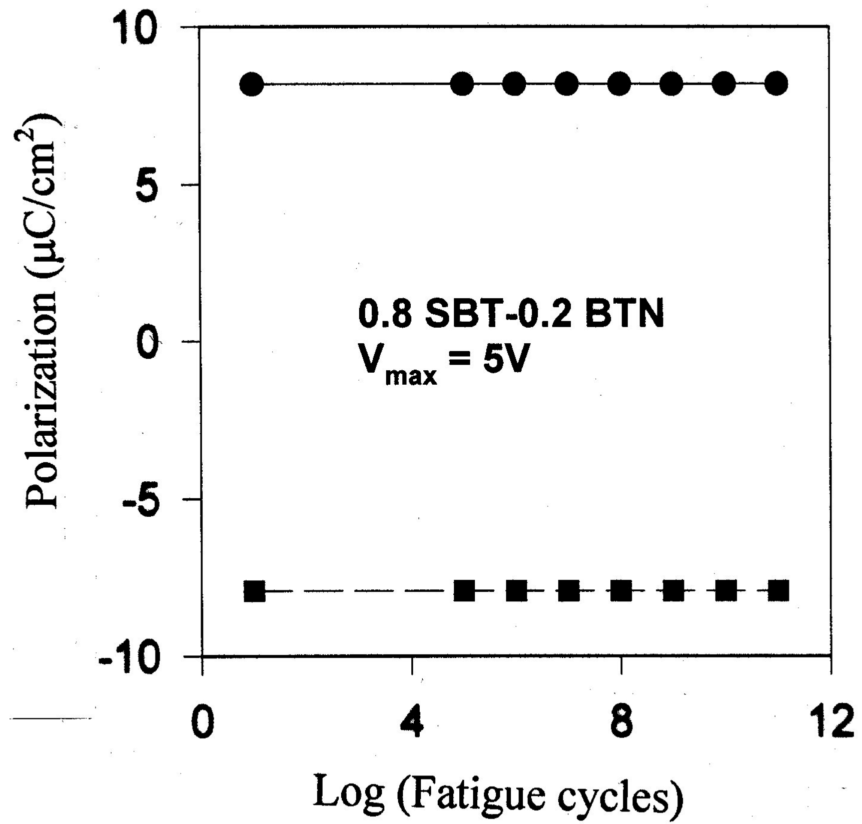

Fig. 7.11. Polarization of 0.25-μm-thick $(SBT)_{0.8}(BTN)_{0.2}$ thim film annealed at 650 ^{0}C for one hour as a function of number of bipolar switching cycles.

Although $SBT_{0.8}BTN_{0.2}$ thin films were found to be superior to SBT thin films in issues of remanent polarization and processing temperatures, the coercive field of $SBT_{0.8}BTN_{0.2}$ (70 kv/cm) was found to be higher than that of SBT (30 kV/cm). However, the operating parameter, which is of practical importance to the semiconductor industry is coercive voltage (V_c), rather than coercive field. In the present study, we have attempted to decrease the V_c by reducing the thickness of the ferroelectric film. To analyze the effect of film thickness on the ferroelectric properties, samples in the thickness range 0.08-0.25 μm with a very smooth surface morphology were prepared by MOSD technique. The ferroelectric properties of $SBT_{0.8}BTN_{0.2}$ thin film capacitors were studied as a function of film thickness and annealing times. Optimum thickness and annealing times were determined which could enable the $SBT_{0.8}BTN_{0.2}$ capacitors be integrated into high density FRAMs. It was observed that as the thickness of the film increased from 0.08 μm to 0.25 μm, the remanent polarization as well as the coercive voltage at a constant applied field of 250 kV/cm increased while the leakage current density decreased as shown in Table 7.3. Well saturated hysteresis loops were obtained even for 0.08 μm thick films, which suggested the suitability of these ultra thin solid solution films for high density FRAM applications. By decreasing the thickness from 0.25 μm to 0.08μm, it was possible to decrease the V_c from 1.6 V to 0.6 V, respectively. The increase in P_r could be attributed to the increase in the number of grains across the cross section with increase in the thickness. The above results show that the combination of solid solution and the MOSD technique were effective in providing excellent ferroelectric properties even in the very thin films of the order of 0.01 μm.

Table 7.3 Variation of remanent polarization (P_r), Coercive voltage (V_c) and leakage current densities (I_L) with thickness of $(SBT)_{0.8}$ $(BTN)_{0.2}$ films annealed at 650 ^{0}C/1 Hr.

Film thickness	**80 nm**	**100 nm**	**250 nm**
P_r (at 250 kV/cm)	4.2 $\mu C/cm^2$	4.5 $\mu C/cm^2$	5.1 $\mu C/cm^2$
V_c (at 250 kV/cm)	0.6 V	0.8 V	1.6 V
I_L (at 250 kV/cm)	8×10^{-5} A/cm^2	10^{-7} A/cm^2	10^{-8} A/cm^2

Table 7.4 shows the dependence of P_r, V_c and leakage current density on the time of annealing. All the three parameters increased with the increase in the time of annealing which could be explained on the basis of grain size dependence on annealing time. Longer annealing times resulted in larger grains and fewer grain boundaries across the cross section. As the grain size increases, the number of unit cells of perovskite phase increases in each grain and hence, it requires a greater coercive field to switch the dipoles from one orientation to the other. Consequently, there was an increase in remanent polarization and coercive voltage with annealing time. The fewer grain boundaries across the cross section possibly account for the increase in the leakage current density. Based on these results, it was found that 0.1-μm-thick $SBT_{0.8}BTN_{0.2}$ films annealed at 650 ^oC for one hour in oxygen atmosphere exhibited the optimum ferroelectric properties. These thin films also showed good fatigue and retention characteristics, similar to SBT thin films. Polarization fatigue was found to be less than 4% even after the application of 10^{10} bipolar switching cycles. The films showed good memory retention (<3%) even after 10^5 seconds of retention time. In summary, 100 nm thick $SBT_{0.8}BTN_{0.2}$ films annealed at 650^0 C for one hour were found to most promising for integration into high density FRAMs.

Table 7.4 Variation of remanent polarization (P_r), coercive field (V_c) and leakage current densities with annealing time of 100 nm thick $(SBT)_{0.8}$ $(BTN)_{0.2}$ films annealed at 650 ^{0}C.

Annealing time (hour)	**1**	**2**	**3**
P_r (at 3V)	4.9 μC/cm^2	6.2μC/cm^2	7.1μC/cm^2
V_c (at 3V)	0.8 V	0.88 V	0.93 V
I_L (at 3V)	10^{-7} A/cm^2	5x10^{-5} A/cm^2	3x10^{-4} A/cm^2

7.5 Conclusions

A successful attempt was made to overcome the problems, such as high processing temperature and low remanent polarization relating to SBT based high density FRAM technology by adapting a solid solution approach. Thin films of $(SBT)_{1-x}(BTN)_x$ solid solution were made by MOSD technique on platinum substrates in the range x = 0.0 to 1.0. Structural and ferroelectric properties of these films were analyzed as a function of annealing temperature (650-750 ^{0}C). While the structure remained similar to SBT, the ferroelectric properties were found to be significantly improved compared to SBT thin films. Both P_r and V_c were found to increase with the increase in the BTN content for each annealing temperature until a maximum was attained and on further addition of BTN, both P_r and V_c decreased. While the maximum was attained at x = 0.4 for the thin films annealed at 700 ^{0}C and 750 ^{0}C, films annealed at 650 ^{0}C showed maximum at x = 0.3. A similar trend was observed in the dielectric constants of these thin films measured at a frequency of 100 kHz, with ε_r varying in the range 80-220. Such a trend of ferroelectric properties was attributed to the grain growth characteristic dependence on annealing temperature and composition. The loss in polarization charge in these capacitors was found to be less than 4% even after 1×10^{10} switching cycles. Based on the above results, optimum ferroelectric properties at a low processing temperature of 650 ^{0}C were obtained at x = 0.2. $SBT_{0.8}BTN_{0.2}$ film processed at 650 ^{0}C exhibited a P_r of 7.0 $\mu C/cm^2$ and a leakage current density less than 10^{-8} A/cm^2, while SBT films processed at the same temperature showed no distinct hysteresis loop at all. However, V_c of 0.25-μm-thick $SBT_{0.8}BTN_{0.2}$ film was found to be as high as 1.6V, which was suitably reduced to

0.8V by reducing the thickness of the films from to 100 nm. The leakage current density was maintained at a low value of 1×10^{-7} A/cm^2 which is comparable to that of SBT thin films. It was further found that 0.1-μm-thick $SBT_{0.8}BTN_{0.2}$ thin films processed at 650 ^{0}C exhibited a low polarization fatigue up to 10^{10} cycles while retaining the stored charge up to 10^5 seconds without any appreciable loss in the switched polarization. These excellent ferroelectric properties of $SBT_{0.8}BTN_{0.2}$ ultra thin film capacitors would enable it to be integrated directly into 1T/1C structure based high density ferroelectric random access memories.

References

1. D. Bondurant and F. Grandinger, IEEC Spec., 30 (1989).
2. S. Dey and R. Zuleeg, Ferroelectrics **108**, 37 (1990).
3. J. F. Scott and C. A. Paz de Araujo, Science **246,** 1400 (1989).
4. J. F.Scott, L. D. McMillas, and C. A. Araujo, Ferroelelctrics **93**, 31 (1989).
5. J. T. Evans and R. Womak, IEEE J. Solid-State Circuits **SSC-23**, 1171 (1988).
6. C. A-Paz de Araujo, J. D. Cuchlaro, L. D. McMillan, M. C. Scott, and J. F. Scott, Nature **374**, 627 (1995).
7. K. Amanuma, T. Hase, and Y. Miyasaki, Appl. Phys. Letters **66**,221 (1995).
8. S. B. Desu, D. P. Vijay, Materials Science and Engineering B **32,** 75 (1995).
9. S. Ohnishi, K. Ishihara, Y.Ito, S. Yokoyama, J. Kudo, and K. Sakiyama, Technical Digest of the IEDM94, **843** (1994).
10. D. J. Taylor, R. E. Jones, P. Zurcher, P. Chu, Y. T. Lii, B. Jiang, and S. J. Gillespie, Appl. Phys. Lett. **68**, 2300 (1996).
11. S. B. Desu and T. K. Li, Materials Science and Engineering B **34**, L4 (1995).
12. Y. Zhu, S.B. Desu, T. K. Li, and S. Ramanathan, J. Mater. Res. **12**, 783 (1997).
13. T. K. Song, J. K. Lee, and H. J. Jung, Appl. Phys. Lett. **69**, 3839 (1996).
14. M. Nagata, D. P. Vijay, X. Zhang, and S. B. Desu, Phys. Stat. Sol. (a) 157, 75 (1996).
15. G. Arlt, D. Hennings, and G. Dewith, J. Appl. Phys. **58**, 1619 (1985).
16. S. B. Desu, C. H. Peng, L. Kammerdiner, and P. J. Schuele, Mater. Res. Soc. Symp. Proc. **200**, 319 (1990).
17. K. Singh, D. K. Bopardikar, and D. V. Atkare, Ferroelectrics **82**, 55 (1988).

18. T. Noguchi, T. Hase, and Y. Miyasaka, Jpn. J.Appl. Phys. **35**, 4900 (1996).

19. Y. Ito, M. Ushikubo, S. Yokoyama, H. Matsunaga, T. Atsuki, T. Yonezawa, and K. Ogi, Jpn. J. Appl. Phys. **35**, 4925 (1996).

20. T. J. Boyle, C. D. Buchheit, M. A. Rodriguz, H. N. Al-Shareef, B. A. Hernandez, B. Scott, and J. W. Ziller, J. Mater. Res. **11**, 2274 (1996).

21. B. Aurivillus, Arkiv Kemi **1**, 463 (1949).

22. E. C. Subba Rao, J. Chem. Phys. **34**, 695 (1961).

23. G. A. Smolenskii, V. A. Isupov and A. I. Agranovskaya, Fiz. Tverd. Tela **3**, 895 (1961).

24. R. E. Newham, R. W. Wolfe, R. S. Hosey, F. A. Dioz-Colon and M. L. Kay, Mater. Res. Bull. **8**, 1183 (1973).

25. X. Zhang, P. Gu and S. B. Desu, Phys. Stat.Sol. (a) **160**, 35 (1997).

26. P. C. Joshi, S. O. Ryu, X. Zhang, and S. B. Desu, Appl. Phys. Lett. **70**, 1080 (1997).

27. E. C. Subba Rao, J. Phys. Chem. Solids **23**, 665 (1962).

28. S. B. Desu, P. C. Joshi, X. Zhang, and S. O. Ryu, Appl. Phys. Lett. **71**, 1041 (1997).